2024 International Conference on Simulation of Semiconductor Processes and Devices (SISPAD) | 979-8-3315-1635-2/24/$31.00 ©2024 IEEE | DOI: 10.1109/SISPAD62626.2024.10733257

Revealing the Noise Dependent Sensitivity of a Junctionless FinFET-based Hydrogen Sensor with Ferroelectric Gate Stack

[1]Navneet Gandhi
VLSI Lab, Electronics & Communication Department
PDPM-IIITDM
Jabalpur, India
21peco03@iiitdmj.ac.in

[2]Sunil Rathore
VLSI Lab, Electronics & Communication Department
PDPM-IIITDM
Jabalpur, India
1912603@iiitdmj.ac.in

[3]Rajeewa Kumar Jaisawal
VLSI Lab, Electronics & Communication Department
PDPM-IIITDM
Jabalpur, India
1912607@iiitdmj.ac.in

[4]P. N. Kondekar
VLSI Lab, Electronics & Communication Department
PDPM-IIITDM
Jabalpur, India
pnkondekar@iiitdmj.ac.in

[5]Naveen Kumar
Device Modelling Group
James Watt School of Engineering
University of Glasgow, UK
naveen.kumar@glasgow.ac.uk

[6]Ankit Dixit
Device Modelling Group
James Watt School of Engineering
University of Glasgow, UK
ankit.dixit@glasgow.ac.uk

[7]Vihar Georgiev
Device Modelling Group
James Watt School of Engineering
University of Glasgow, UK
vihar.georgiev@glasgow.ac.uk

[8*]Navjeet Bagga
School of Electrical and Computer Sciences
Indian Institute of Technology
Bhubaneswar, India
navjeet@iitbbs.ac.in

***Abstract*—This paper reveals the role of Flicker (1/*f*) Noise and process variations (*i.e.*, random dopant fluctuation, RDF) on the sensitivity of the Junctionless FinFET-based hydrogen gas (H_2) sensor with a ferroelectric (FE) gate stack, which offers the privilege of Negative Capacitance (NC) effect. In general, the FE-stack has two possible configurations, i.e., MFMIS and MFIS. Therefore, the sustainability and selectivity of both configurations under the influence of Noise on the sensor's sensitivity have been thoroughly investigated using well-calibrated TCAD models. With varying H_2 concentrations (in ppm) and FE thicknesses in both configurations, the acquired electrical characteristics, sensing metrics, and noise spectral density (S_{IDS}) reveal that the MFMIS is an appropriate choice for realizing a FET-based sensor.**

Keywords*— Hydrogen gas, Junctionless, Negative Capacitance Flicker Noise, Sensitivity.

I. Introduction

Embedding the ferroelectric layer at the gate stack of the conventional MOS results in the NC phenomenon, when/if the FE thickness and Landau parameters are adequately tuned [1]. Therefore, realizing an FE-based FET provides a suitable pathway to achieve channel conductivity modulation, which, in turn, promotes FE-stacked transistors as a potential candidate for sensing applications. Among all possible FET-based sensors, the gas sensors are of prime importance and require a low-cost, portable, noise-immune, and sustainable design. It is crucial to detect gases like hydrogen (H_2), phosphine (PH_3), ammonia (NH_3), etc. with high sensitivity and accuracy [2]. This paper chooses the hydrogen gas (H_2) sensor design using Junctionless FinFET, which offers an additional advantage over baseline FinFET [3]-[6]. Unlike conventional MOSFET, the Junctionless (JL) transistors are particularly promising due to their straightforward fabrication and reduced sensitivity to surface roughness scattering [7]. Further, the choice of JL FinFET mitigates short-channel effects and requires less steep doping profiles, making it well-suited for nanoscale non-planar sensitive devices. Thus, transistor characteristics could be retrieved for realizing a sensor. The additional advantage in sensing characteristics could be realized by incorporating NC merits using an embedded FE layer. In general, the FE-stack has two possible configurations, i.e., MFMIS and MFIS [8]. MFMIS is not a reliable and widely opted configuration owing to the presence of an internal metal; however, it is a good configuration for studying the modeling behavior of the device. On a similar ground, MFIS is a widely accepted configuration due to CMOS compatible design. Therefore, as far as this transcript is concerned, we investigated the best-suited configuration for noise-immune and sustainable sensor design.

II. Device Structure and TCAD Setup

Sentaurus TCAD [9] is employed for investigating the electrical and Noise characteristics of the proposed JLNC FinFET for two configurations (MFMIS and MFIS). In our previous publication [10], the JL FinFET (Fig.3a) is fabricated and characterized for the transient response for H_2 detection. The same (Fig.3b) is opted for simulation and calibrated against the available experimental data [11], which ensures the credibility of our simulation setup. To subside the series resistance and RDF, fixed n-type doping is considered in the source/drain and channel region. The two possible FE-stack configurations are embedded over the baseline JL FinFET to realize the JLNC FinFET-based sensor (Fig.2a-b). The S-curve obtained (Fig.2d) from TCAD is used to validate the L-K parameters, confirming that it aligns with the NC region for a 1.8nm FE thickness (T_{FE}) [12]. Table I comprises the default parameters used in the simulation unless stated otherwise.

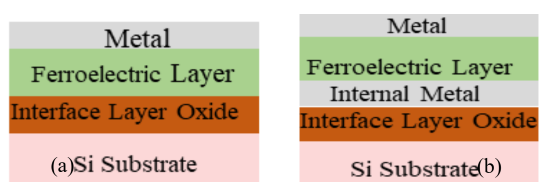

Fig.1 Schematic of (a) metal ferroelectric insulator semiconductor (MFIS) and (b) metal ferroelectric metal insulator semiconductor (MFMIS) capacitor. This is used to realize Junctionless Negative Capacitance (JLNC) FinFET-based H_2 sensor.

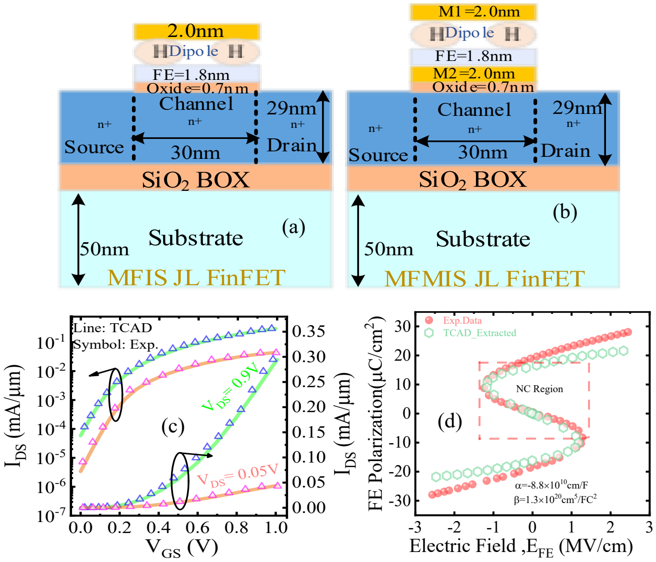

Table-I Parameter Table

Parameter	Value	Parameter	Value
Fin Height	29nm	Doping Conc.	$2*10^{19}$ cm^{-3}
Fin Width	10nm	EOT	1nm
Metal WF	5.05eV	BOX Thickness	10nm

Fig.2 Cross-sectional view of the JLNC FinFET realized by (a) MFIS configuration; and (b) MFMIS configuration of the gate-stack. (c) calibration of the baseline JL FinFET, and (d) extraction of the S-curve for MFIM capacitor for corresponding L-K parameter shown inside the figure. Table-I: Parameter Table.

III. Fabrication Steps and Sensing Mechanism

The basic fabrication steps for the baseline JL-FinFET are shown in the flow chart-I (Fig.3). We used a doped-high-k material as the ferroelectric (FE) layer, applying the L-K model to operate the device in the negative capacitance (NC) region. This JLNC device is designed for H_2 gas sensing applications. Hydrogen, a gas that is colorless, tasteless, and odorless, presents safety risks due to its high combustion rate and rapid burning velocity, making quick leak detection crucial. Normally, hydrogen gas consists of diatomic molecules, each made up of two hydrogen atoms bonded by covalent interactions. In the transduction mechanism, hydrogen molecules dissociate and adsorb onto the palladium metal gate surface. The gas sensing methodology for the proposed sensor is depicted in the flow chart II (Fig.3). The effect of varying H_2 concentration, i.e., 1.0ppm to 1.005ppm has been investigated considering the H_2 gas diffuses over gas sensing elements (i.e., gate metal) of the JLNC FinFET with two FE-stack configurations. The change in H_2 conc. effectively tunes the metal work function (WF) and, in turn, the channel conductivity (Fig.3c). Thus, the significance of varying H_2 concentration is visible in the electrical characteristics of the proposed JLNC FinFET.

Table II Surface Concentration of H_2 at 1.0ppm

Conc.	Conc.(gm/l)	Molar Conc (M/l)	$H_{Surf}=q_H\times$molar Conc.× Avogadro no. (charge per cm^3)
1.0ppm	0.001	4.96×10^{-4}	5.9748×10^{20}
q_H =No. of atoms/proton charge =2			

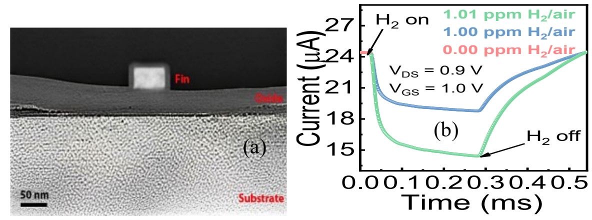

Flow Chart-I

Step1: The device was created on a p-type Si/SiO2 substrate featuring a thermally grown oxide layer measuring 500nm. Electron beam lithography was then employed for patterning, followed by mass-assisted etching.

Step2: All Thickness measurements were conducted utilizing an optical profilometer, while the device structure underwent examination using a field emission scanning microscope (FESM-ZEISS).

Step3: Metal contact was applied through electron beam evaporation. Sensing experiments took place within customized gas sensor characterization equipment, which was connected to a semiconductor device analyzer (Agilent B1500A)

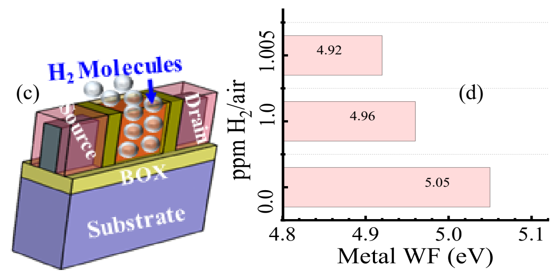

Flow Chart II

Step1: The variation in the metal gate work function, with respect to the concentration of the hydrogen gas, represents as

$$\Delta\emptyset_m = M_q - \left[\left(\frac{RT}{4F}\right) * In(P)\right]$$

Here, 'R' is the gas constant=8.314 JM^{-1}K^{-1}, 'T' is ambient temperature=300K, 'F' is Faraday's constant=96500CM^{-1}, and P is partial pressure of gas (P=2.5Pa).

Step2: Then, effective metal gate work function after diffusion of hydrogen gas molecules is

$$\emptyset_{meff} = \emptyset_m \pm \Delta\emptyset_m$$

$\emptyset_m$ is the work function of reference device

Step3: Assume that all hydrogen atom at the adsorption site of metal surface reached at the interface adsorption site (A_{Int}). Then

$$A_{Int} = H_{Surf}$$

For 'X' ppm conc. of the hydrogen gas, is equivalent to 0.001*X gm/l. Dividing gm/l by molecular mass of hydrogen=2.016gm/mol then it gives molar concentration of hydrogen (M/l) for 'X' ppm

$$M_q=0.001\times H_{Surf}$$

Fig.3 (a-b) SEM image, and the transient response of the fabricated Junctionless FinFET. The figures are already presented in our previous publication [5]. (c) *3D* schematic of the proposed JL FinFET, and (d) WF variation with varying H_2 concentration.

IV. Results and Discussion

The significance of varying H_2 conc. is visible in the electrical characteristics of the proposed JLNC FinFET. I_{DS}-V_{GS} plot for baseline JL FinFET and JLNC FinFET with MFMIS and MFIS configurations (Fig.4a) shows that JLNC designs exhibit lower OFF current compared to the baseline device.

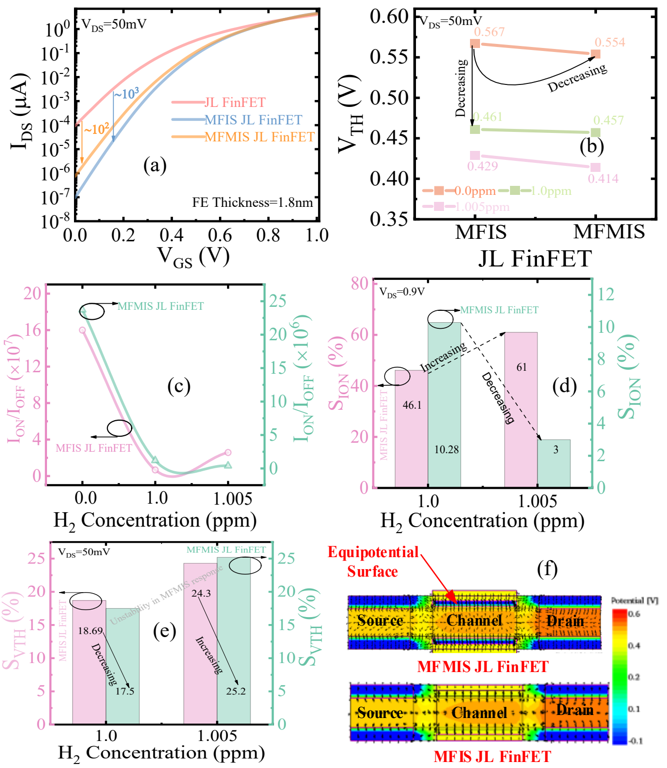

Fig.4 (a) comparison plot of I_{DS}-V_{GS} characteristic of the baseline Junctionless FinFET with MFMIS and MFIS based Junctionless FinFET structure, (b-c) V_{TH} and I_{ON}/I_{OFF} variation at different H_2 concentrations (in ppm) for both configurations, respectively, (d-e) V_{TH} sensitivity and I_{ON} current sensitivity variation, respectively, for proposed sensor, and (f) electrostatic potential distribution at 0.0ppm for both device along the fin direction.

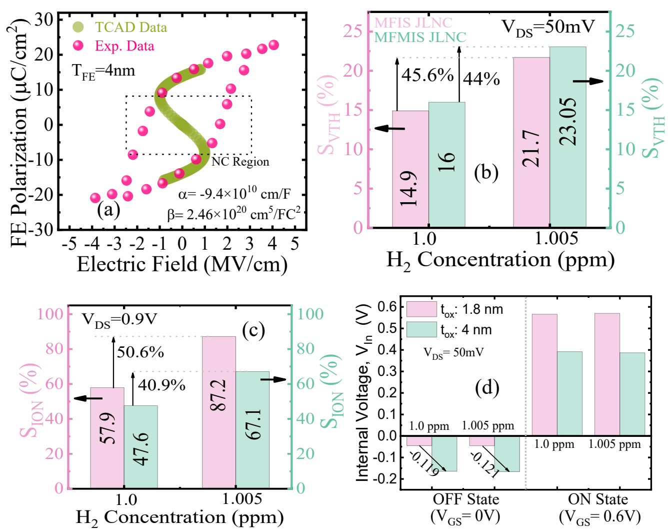

Fig.5 Response analysis of the proposed H_2 sensor at different concentrations (in ppm) with an FE thickness of 4nm for both MFIS and MFMIS configurations. Here (a) calibration of S curve for 4nm Zr doped HfO_2 FE material [13] using *Sentaurus* TCAD [9], (b-c) sensitivity analysis for the proposed sensor both threshold voltage and ON current, respectively. (d) variation in inner metal gate voltage in MFMIS for varying H_2 concentrations. This shows the MFMIS structure has good sensing ability, which promotes the choice of the MFMIS configuration.

Table III

Percentage increase in S_{IDS} at 1.005ppm with respect to 1.0ppm

Device	T_{FE}=1.8nm	T_{FE}=4nm
MFIS JLNC FinFET	526.7%	737.30%
MFMIS JLNC FinFET	523.52%	109%

However, due to instability caused by residual charges on the internal metal plate, the MFMIS JLNC FinFET has a higher leakage current than the MFIS counterpart. The change in the threshold voltage (V_{TH}) and current ratio (I_{ON}/I_{OFF}) of the proposed sensor with varying gas concentration (Fig.4b-c) reveals that the leakage current from the internal metal gate can cause instability in the NC region of MFMIS-based sensors, leading to fluctuations in their sensitivity. The sensitivity (S_{ION}, S_{VTH}) of the proposed sensor (Fig.4d-e) illustrates that V_{TH} sensitivity is higher in the MFIS JLNC FinFET.

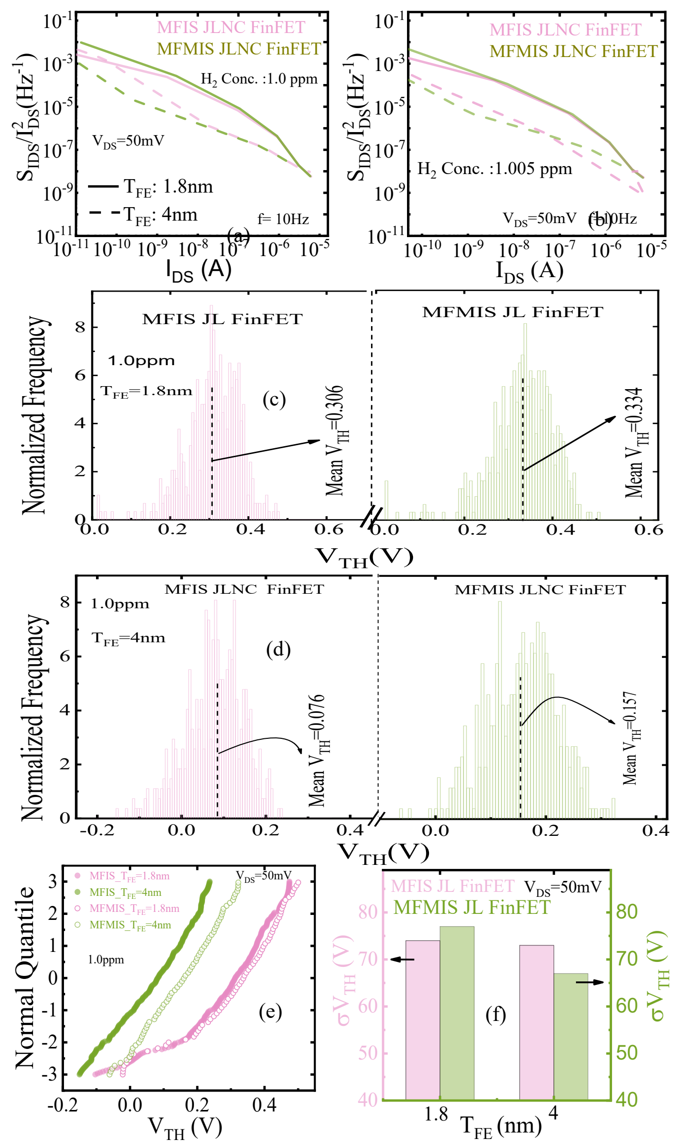

Fig.6 Represent the flicker noise spectral density for varying H_2 conc. (a) 1.0ppm, and (b) 1.005ppm. (c-d) variation of threshold voltage for 50 discrete random samples at T_{FE} of 1.8nm and 4 nm, respectively, (e) Normal Quantile plot at 1.0ppm for different thicknesses, and (f) standard deviation of V_{TH}.

The distribution in the electric field vector across the fin direction shows the internal voltage amplification in MFMIS (Fig.4f). The performance of the proposed sensor is investigated with varying T_{FE} (i.e., 1.8nm and 4nm). S-curve for T_{FE}= 4nm is also calibrated against the experimental data [13] (Fig.5a). At higher T_{FE}, the FE capacitance decreases, while internal amplification gain increases. This results in a significant reduction in OFF current (I_{OFF}). MFMIS architecture demonstrates a more stable response compared to devices with lower T_{FE} thickness. Furthermore, the V_{TH} sensitivity tends to decrease with increasing T_{FE} while its I_{ON} sensitivity shows an increasing trend (Fig.5b-d). To analyze the low-frequency noise behavior, the noise spectral density with varying T_{FE} and H_2 conc. is plotted (Fig.6a-b). JL devices use a high metal gate WF to create a positive charge in the channel and a negative charge on the internal metal gate. As T_{FE} increases, more negative charge accumulates on the internal gate, leading to a higher negative voltage. Thus, the results reveal that as H_2 concentration increases, the effect of flicker noise becomes more pronounced. Furthermore, at higher T_{FE}, the impact of flicker noise is lower in MFMIS than in the MFIS JLNC FinFET (Table III). Further, we investigated the impact of the RDF for different H_2 conc., showing a significant variation in V_{TH} (Fig.6c-d) around its mean value. Thus, at higher H_2 conc. the effect of RDF increases and also this effect reduces at higher thickness for MFMIS. There is a nonlinear fit in the quantile plot (more tilt) of V_{TH} for 1.0 ppm for T_{FE}=1.8nm (Fig.6e), which tilts further as the H_2/air conc. increases. Variation in the standard deviation of V_{TH} is shown in Fig.6f.

V. Conclusion

Using well-calibrated TCAD models, we investigated the performance of a ferroelectric stacked Junctionless FinFET-based H_2 gas sensor. The two possible choices of FE-stack, i.e., MFMIS and MFIS have been analyzed for electrical and noise analysis with varying H_2 concentrations. The sensitivity of the proposed sensor has been investigated using V_{TH}, $I_{OFF,}$ and I_{ON}/I_{OFF}, as sensing metrics. Where our revealing found that at higher gas concentrations the effect of flicker noise and RDF increases, and along with higher FE thickness impact of flicker noise and RDF is less in MFMIS JLNC FinFET compared to the MFIS JLNC FinFET architecture. MFMIS is a more sustainable choice for noise-immune sensor design.

Acknowledgment

Navjeet Bagga would like to acknowledge the support received from CSIR HRDG-II, project no. 22/0896/23.

References

[1]. R. K. Jaisawal, S. Rathore, P. N. Kondekar, and N. Bagga, “Reliability of TCAD study for HfO2-doped Negative capacitance FinFET with different Material-Specific dopants,” *Solid. State. Electron.*, vol. 199, Jan. 2023, doi: 10.1016/j.sse.2022.108531.

[2]. I. Lundström, S. Shivaraman, C. Svensson, and L. Lundkvist, “A hydrogen-sensitive MOS field-effect transistor,” *Appl. Phys. Lett.*, vol. 26, no. 2, pp. 55–57, Jan. 1975, doi: 10.1063/1.88053.

[3]. N. Gandhi, R. K. Jaisawal, S. Rathore, P. N. Kondekar, and N. Bagga, “A proof of concept for reliability aware analysis of junctionless negative capacitance FinFET-based hydrogen sensor,” *Smart Mater. Struct.*, vol. 33, no. 3, Feb. 2024, doi: 10.1088/1361-665X/ad2028.

[4]. S. Rathore *et al.*, “Self-Heating Aware Threshold Voltage Modulation Conforming to Process and Ambient Temperature Variation for Reliable Nanosheet FET,” *IEEE Int. Reliab. Phys. Symp. Proc.*, vol. 2023-March, May 2023, doi: 10.1109/IRPS48203.2023.10117918.

[5]. R. Kumar Jaisawal, S. Rathore, P. N. Kondekar, and N. Bagga, “Unveiling the reliability of negative capacitance FinFET with confrontation of different HfO2-ferroelectric dopants,” *Solid. State. Electron.*, vol. 215, May 2024, doi: 10.1016/j.sse.2024.108896.

[6]. N. Gandhi *et al.*, "Sensitivity and Reliability Assessment of a Strained Silicon Junctionless FinFET-based Hydrogen Gas Sensor," *2024 IEEE Latin American Electron Devices Conference (LAEDC)*, Guatemala City, Guatemala, June 2024, pp. 1-4, doi: 10.1109/LAEDC61552.2024.10555835.

[7]. S. Sahay and M. J. Kumar, “Insight into Lateral Band-to-Band-Tunneling in Nanowire Junctionless FETs,” *IEEE Trans. Electron Devices*, vol. 63, no. 10, pp. 4138–4142, Aug. 2016, doi: 10.1109/TED.2016.2601239.

[8]. G. Pahwa, A. Agarwal, and Y. S. Chauhan, “Numerical Investigation of Short-Channel Effects in Negative Capacitance MFIS and MFMIS Transistors: Subthreshold Behavior,” *IEEE Trans. Electron Devices*, vol. 65, no. 11, pp. 5130–5136, Nov. 2018, doi: 10.1109/TED.2018.2870519.

[9]. Synopsys 2019, Sentaurus Device User Guide (Mountain View, CA: Synopsys, Inc.

[10]. N. Gandhi, S. Rathore, R. K. Jaisawal, P. N. Kondekar, S. Dey, and N. Bagga, “Unveiling the Self-Heating and Process Variation Reliability of a Junctionless FinFET-based Hydrogen Gas Sensor,” *IEEE Sensors Lett.*, Aug. 2023, doi: 10.1109/LSENS.2023.3309263.

[11]. R. Rios *et al.*, “Comparison of junctionless and conventional trigate transistors with L g down to 26 nm,” *IEEE Electron Device Lett.*, vol. 32, no. 9, pp. 1170–1172, Jul. 2011, doi: 10.1109/LED.2011.2158978.

[12]. M. Hoffmann, B. Max, T. Mittmann, U. Schroeder, S. Slesazeck, and T. Mikolajick, “Demonstration of High-speed Hysteresis-free,” pp. 727–730, Dec. 2018,doi: 10.1109/IEDM.2018.8614677.

[13]. X. Lyu, M. Si, X. Sun, M. A. Capano, H. Wang, and P. D. Ye, “Ferroelectric and Anti-Ferroelectric Hafnium Zirconium Oxide: Scaling Limit, Switching Speed and Record High Polarization Density,” *Dig. Tech. Pap. - Symp. VLSI Technol.*, vol. 2019-June, pp. T44–T45, July 2019, doi: 10.23919/VLSIT.2019.8776548.